

A novel flame retardant system of AMP and KH570-modified silica sol for cotton fabrics

Mengwei Liu¹, Fei You^{1,2*}, Qianyu Lu¹, Zhenhua Wang¹, Yuli Zhang¹ and Hao Huang¹

¹ College of Safety Science and Engineering, Nanjing Tech University, Nanjing 211816, China

² Institute of Fire Science and Engineering, Nanjing Tech University, Nanjing 211816, China

* Corresponding author, E-mail: fyounjtech.edu.cn

Abstract

Tetraethoxysilane (TEOS) and γ -(methacryloyloxy) propyltrimethoxysilane (KH570) were used to prepare a single silica (SiO_2) sol and a silica-5'-adenosine monophosphate (AMP, bio-based substance) hybrid sol via sol-gel processes. Then, the prepared series of sols were successively applied onto the cotton fabric (COT) surface through a dipping-baking method. Fourier infrared spectroscopy (FTIR), X-ray photoelectron spectroscopy (XPS), X-ray diffraction (XRD), scanning electron microscope (SEM), energy dispersive spectroscopy (EDX), thermogravimetric analysis (TGA), limiting oxygen index (LOI), vertical flammability test (VFT), and cone calorimetry test (CCT) were used to characterize the functional groups, surface element compositions, crystal structures, microscopic morphologies and surface element distributions, thermal stability and flame retardancy levels of original (raw), and treated cotton fabrics. Results show that the series of sols are successfully converted to gels and coated onto the cotton fabric surfaces. AMP- SiO_2 -KH570@COT shows the best flame retardancy with the highest char residue rate (48.7%) (6.5 times that of raw cotton fabric), and a LOI value of 27.7% (non-flammable level). It can self-extinguish with a char length of only 8.2 cm in a VFT. It shows reduced total heat release (THR) and peak heat release rate (PHRR) by 3.8% and 48.5% and has the longest ignition time (43 s) in a CCT. The SiO_2 sol-converting gel modified with KH570 clearly improves the interfacial compatibility with the cotton fabric and effectively isolates heat and oxygen. Meanwhile, the AMP gel pyrolyzes the phosphate group at high temperatures to accelerate the carbonization degrees of cotton fibers. These components show good synergistic flame-retardant effects.

Citation: Liu M, You F, Lu Q, Wang Z, Zhang Y, et al. 2025. A novel flame retardant system of AMP and KH570-modified silica sol for cotton fabrics. *Emergency Management Science and Technology* 5: e004 <https://doi.org/10.48130/emst-0025-0002>

Introduction

As living standards continue to rise, the demand for textiles in daily life has been steadily increasing^[1,2]. However, according to reports, quite a few fires related to textiles occur every year and cause considerable casualties and economic property losses^[3]. For example, on November 20, 2023, a large fire accident occurred in Wuxi Tiantianrun Textile Technology Co. Ltd., (China) where the high-temperature operation of machinery ignited cotton fibers and other combustibles, resulting in seven deaths of persons and a burnt fire area of about 5,100 m²^[4]. Among all textiles, cotton fabrics are widely used in the automotive industry, protective clothing, military applications, and daily essentials due to their lower-price, softness, air permeability, biodegradability, and excellent mechanical durability^[5,6]. However, cotton typically exhibits an LOI value of 18.0%, indicating it is an inflammable and potentially hazardous material^[7–9]. Consequently, enhancing the fire resistance of cotton fabrics has emerged as a critical research focus^[10,11]. Halogen-based flame retardants are among the earliest-developed flame retardant products. However, they produce toxic and harmful substances during combustion, leading to environmental pollution, and endangering human health^[12,13]. Phosphorus-based flame retardants also face multiple challenges of poor compatibility, low thermal stability, large smoke generation, and high volatility. For example, organophosphorus flame retardants such as Pyrovatex CP and Proban are effective, but the N-CH₂-OH group they contain can release formaldehyde and other harmful substances, potentially leading to further environmental pollution^[14,15].

To align with global green strategies, researchers have increasingly focused on nitrogen-based, silicon-based, and phosphorus-nitrogen-silicon synergistic flame retardants. These alternatives are

primarily designed to be halogen-free and environmentally friendly. In this context, bio-based flame retardants have emerged as promising options, offering both effective flame retardancy and enhanced environmental sustainability^[7,16]. Their acceptable flame-retardant properties stem from their molecular compositions and structures, as well as their abilities to form stable char layers under high temperatures or fire conditions^[17]. Some renewable and sustainable biological macromolecules, such as phytic acid (PA), deoxyribonucleic acid (DNA), protein, chitosan, starch, cyclodextrin, sodium alginate (SA), have been identified as promising flame retardant candidates^[18–20]. Alongi et al.^[21] first explored the use of DNA extracted from herring sperm as a novel flame retardant system, demonstrating the improved thermal stability and flame retardant properties of cotton fabrics. However, the high cost of DNA limits its large-scale applications; Wang et al.^[22] developed a bio-based coating composed of adenosine triphosphate (ATP), chitosan, and polyethyleneimine on a lyocell fabric through a layer-by-layer (LBL) self-assembly method. The resulting lyocell fabric exhibits optimal flame retardancy. AMP, a nucleotide found in ribonucleic acid (RNA), is rich in N and P elements and cost-effective. However, it is seldom used for flame retarding cotton fabrics till now. Moreover, biological materials are inherently unstable. Modifications are required to enhance their performances. Further researchers prefer to combine flame-retardant elements, such as phosphorus, nitrogen, silicon, and boron, with biomass and improving their compatibility^[23].

In this study, a series of flame-retardant and environmentally friendly functional cotton fabrics were developed by incorporating AMP with a SiO_2 sol using sol-gel plus dipping-baking (drying) processes. Specifically, the SiO_2 sol was synthesized under acidic conditions and subsequently modified with KH570. A 20.0 wt% AMP

sol and SiO₂-KH570 sol were sequentially applied to the cotton fabrics. The microscopic morphologies, internal chemical structures, element distributions, and crystal structures of the series-treated fabrics were characterized by SEM, FTIR, XPS, and XRD techniques. The thermal stability and flame retardancy of the fabrics were evaluated through TGA, LOI, VFT, and CCT techniques. The flame retardant effects of bio-based AMP and KH570-modified SiO₂ sol (double-layer coating system), as well as their synergistic mechanisms, were explored.

Materials and methods

Materials

Pure cotton fabric (111 g/m²) was provided by Nanjing Qicai Mei Textile Company (Nanjing, China). AMP (AR, ≥ 99.0%) was acquired from Shanghai Aladdin Reagent Co., Ltd (Shanghai, China). Hydrochloric acid (HCl, AR, 37.0%) was obtained from Shanghai Pilot Chemical Co., Ltd (Shanghai, China). KH570 (IR, ≥ 99.0%), and TEOS (AR, ≥ 35.0%) were acquired from Sinopharm Chemical Reagent Co., Ltd (Shanghai, China). Anhydrous ethanol (EtOH, AR, ≥ 99.6%) was obtained from Wuxi Yasheng Chemical Co., Ltd (Wuxi, China). Deionized water (H₂O, IR, ≥ 99.9%) was provided by Nanjing Wanqing Chemical Glassware Instrument Co., Ltd (Nanjing, China). Hydrochloric acid (HCl, AR, 37.0%) was obtained from Shanghai Pilot Chemical Company (Shanghai, China). All reagents were used as described upon receipt. The molecular structures of TEOS, KH570, and AMP are presented in Table 1.

Sample preparation

Preparation of AMP sol

Fourty grams of AMP powder and 160.0 g of deionized water were weighed and mixed. The resulting mixture was transferred to a thermostatic magnetic stirrer (model 78HW-1, Ronghua Instrument Manufacturing Co., Ltd., Changzhou, China) and stirred. The pH was adjusted to 6.0 by adding a 10.0 wt% NaOH solution until a colorless and transparent AMP sol was obtained.

Preparation of SiO₂ sol

A mixture of TEOS, EtOH, and H₂O was prepared in a molar ratio of 1:2:6 (TEOS : EtOH : H₂O), with a small amount of HCl added as an acidic catalyst. The pH of the mixture was adjusted to 6.0, and it was stirred at 60.0 °C for 3 h to allow hydrolysis and condensation. The mixture eventually became a transparent and clear sol.

Preparation of SiO₂-KH570 hybrid sol

KH570 was used as a surface chemical modifier to enhance the aggregation of SiO₂ particles and improve the compatibility between the SiO₂ nanoscale network and cotton fibers. The optimal dispersibility of sol particles was achieved when the mass ratio of

SiO₂ sol to KH570 is 9:1. At room temperature, 20.0 g of KH570 was added to 180.0 g of SiO₂ sol. The mixture was then stirred at 60.0 °C for 1 h to obtain the KH570-modified SiO₂ sol. The process diagram of SiO₂-KH570 hybrid sol is shown in Fig. 1.

Pre-treatment processes for cotton fabrics

To remove impurities and chemical residues from the cotton fabric surface, the fabrics were initially immersed in deionized water at 100.0 °C for 30 min. The fabrics were then rinsed with deionized water until the wash solution became clear. Afterward, the fabrics were air-dried in a well-ventilated area and dried in a constant temperature oven (model PHG-9036A, Shanghai Jinghong Experimental Equipment Co., Ltd., Shanghai, China) at 80.0 °C before use.

Finishing processes of hybrid and doped sols on cotton fabrics

The pretreated cotton fabrics were individually immersed in the AMP sol and SiO₂-KH570 sol for 10 min each. After the first impregnation, the samples were removed, air-dried, and cured at 60.0 °C for 30 min. They were then dipped again into the respective sols and air-dried once more, followed by curing at 80.0 °C for 2 h. The preparation process of AMP-SiO₂-KH570 hybrid sol for the finishing cotton fabrics is shown in Fig. 1. Additionally, cotton fabric samples with composite double coatings of unmodified SiO₂ sol and AMP sol were also prepared.

Testing and characterization

The particle size distribution of a series of silica-based sol systems was measured using a Mastersizer 2000 laser diffraction particle size analyzer (Malvern Instruments Ltd., UK), with distilled water serving as the dispersant.

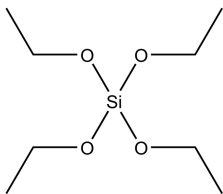
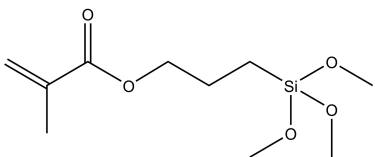
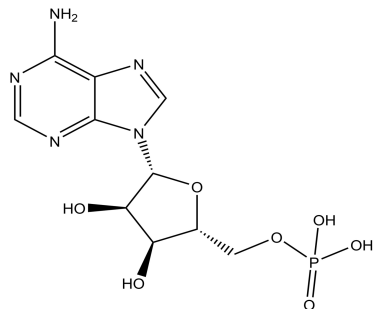
Surface morphologies and elemental compositions of the cotton fabrics and their char residues after VFT were analyzed using a ZEISS Gemini 300 scanning electron microscopy (SEM, Carl Zeiss Co., Ltd., Germany) coupled with energy dispersive X-ray spectroscopy (EDX, max20 EDX mapping module, Oxford Instrument Technology Co., Ltd., Shanghai, China). SEM imaging was performed with an accelerating voltage at 5 kV under vacuum conditions. Before testing, all treated samples were gold-coated.

X-ray photoelectron spectroscopy (XPS, K-Alpha+, Thermo Fisher Scientific Co., Ltd., Waltham, USA) was employed to analyze the surface elemental composition. The fabric samples (5 × 5 mm² each) were cut and adhered to conductive carbon tapes.

Fourier transform infrared (FTIR) spectra of all the samples were recorded using an IS5 FTIR spectrometer (Thermo Fisher Scientific Co., Ltd., Shanghai, China) via the KBr pellet technique, within the range of 4,000–400 cm⁻¹. Each sample was scanned 32 times at a resolution of 4 cm⁻¹.

X-ray diffraction (XRD) patterns of cotton fabric samples were obtained with a D8 Advance photoelectron spectrometer (Bruker

Table 1. The molecular structures: TEOS, KH570, and AMP.

Substance	TEOS	KH570	AMP
Structure			

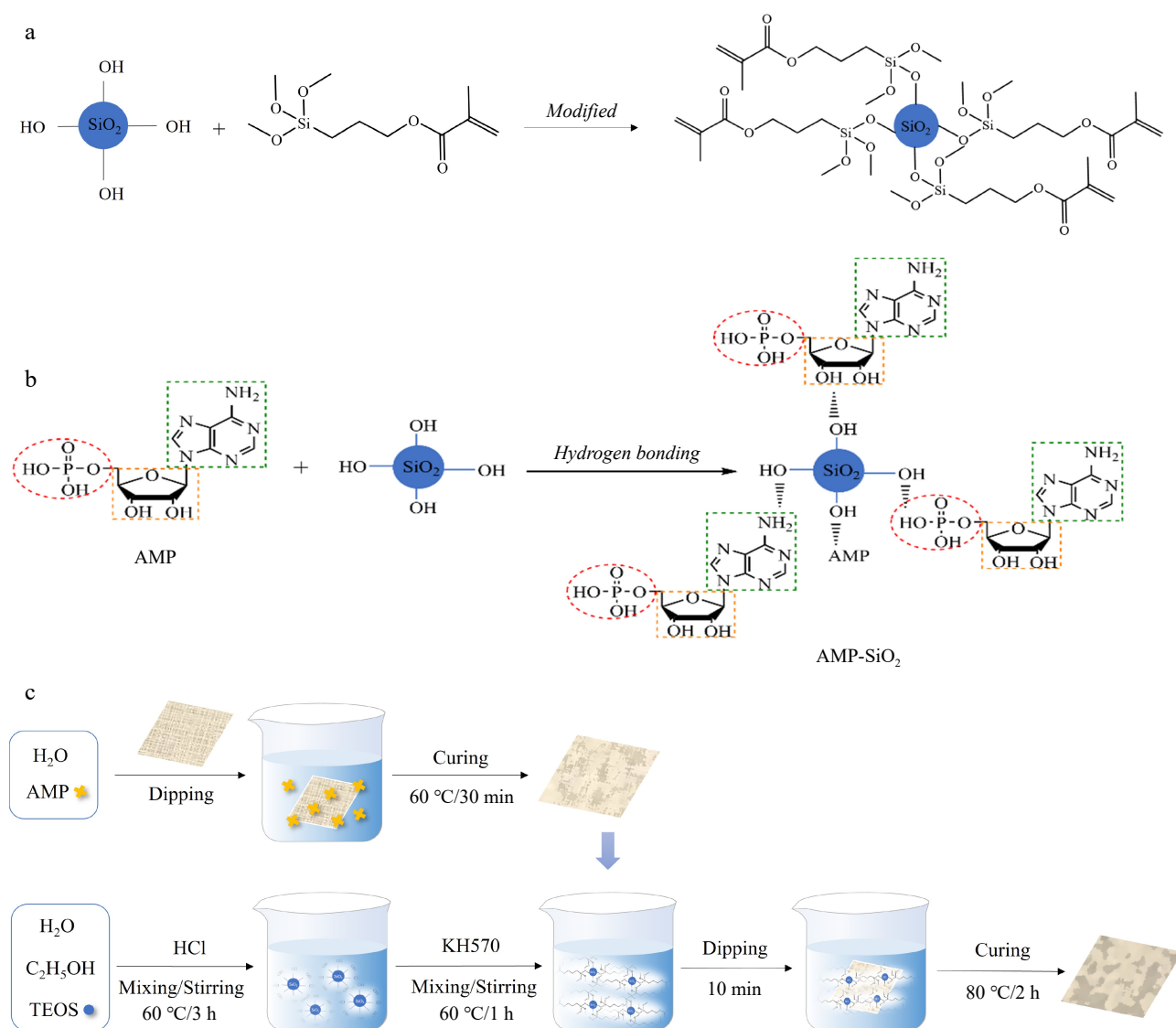


Fig. 1 (a) Path diagram of SiO₂-KH570, (b) synthetic route of an AMP-SiO₂ sol, (c) preparation process of AMP-SiO₂-KH570@COT.

Co., Ltd., Germany) using CuK α radiation at 36 kV and 20 mA, operating at room temperature. The scattering angles ranged from 10° to 50°. By observing the diffraction patterns, whether the treatments have altered the crystal structures of the cotton fibers can be judged. It is crucial for understanding the interaction between the flame retardant coatings and the cotton substrate.

The thermal stability analysis was performed under N₂ atmosphere using a TGA/DSC3+ (Mettler Toledo, Columbus, USA). Approximately 10.0 mg of each sample was tested from 30.0 to 700.0 °C at a N₂ flowing rate of 50 mL/min and a heating rate of 10 °C/min.

The LOI values of cotton fabrics were measured according to the Chinese standard of GB/T 5454-1997^[24], using a JF-3 oxygen index meter (model ZY6155A, Zonsky Instrument Co., Ltd., Dongguan, China.) with samples sized 150 × 58 mm².

The VFT of raw and treated cotton fabric samples (300 × 89 mm²) were conducted according to the Chinese standard of GB/T 5455-2014^[25], with a VFT tester (model CZF-5CD 50 W, Tianjin Xunyu Technology Co. Ltd., Tianjin, China).

The combustion properties of cotton fabrics were assessed using a FTT0007 cone calorimeter (Fire Testing Technology Ltd., East

Grinstead, UK), according to the ISO 5660-1 standard^[26]. A three-layer cotton fabric sample (100 × 100 mm² each) was wrapped in a sheet of aluminum foil and positioned in a metal grid holder, exposed to a radiative heat flux of 35 kW/m².

Results and discussion

Particle size distribution of SiO₂ sol and SiO₂-KH570 sol

As shown in Fig. 2, compared to SiO₂ sol, the SiO₂-KH570 sol particles are uniformly dispersed, and the overall size distribution is shifted toward smaller sizes. This shift occurs because KH570 and SiO₂ combine through hydrogen bonding, with the long-chain molecules on the surface of the particles winding and cross-linking, resulting in a certain degree of steric hindrance. Consequently, the original silica sol cannot densely spread on the surface of cotton fabrics^[27]. Therefore, the re-aggregation phenomenon has improved significantly. In addition, due to the soft organic segments in the structure of KH570, the cotton fabric treated with SiO₂-KH570 sol has a softer handle, better dispersibility, and stability than cotton fabric treated with SiO₂ sol.

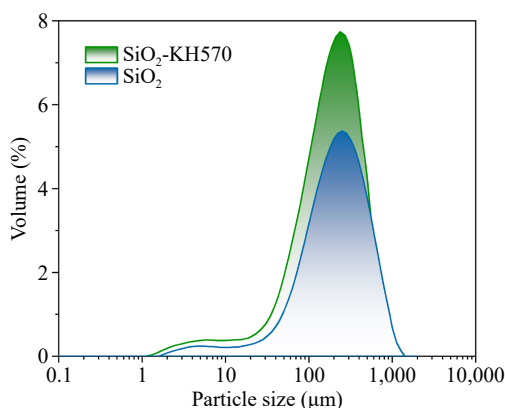


Fig. 2 Particle size distribution of SiO_2 sol and SiO_2 -KH570 sol.

Microscopic morphology and element content analysis

Figure 3 displays the SEM images of raw and sol-finished fabrics, with a magnification of 800 times.

As illustrated in Fig. 3, the raw cotton fiber exhibits a smooth surface and is individually interwoven, forming a twisted ribbon structure through helical winding. For SiO_2 @COT, the SiO_2 sol forms a uniform coating on the cotton surface, exhibiting strong adhesion. This can be attributed to the structure of cotton fiber, which consists of single-cell seed cellulose. Its hollow interior and twisted, porous surface provide an excellent substrate for the adsorption of numerous ultrafine SiO_2 sol particles^[28]. In contrast, after treatment with the AMP coating, the surface adhesion is less pronounced, indicating that the SiO_2 sol exhibits a stronger effect than AMP sol in terms of physical adhesion and chemical hydrogen bond adsorption. For AMP- SiO_2 @COT, the interconnection effect of each single fiber is significantly enhanced due to the hydrogen bond between the dual coatings, leading to fewer grooves and spaces. As can be seen from Fig. 3, small cracks are observed on the surface of the SiO_2 -KH570@COT, which form during the curing process of the gelled sol coating. However, due to the strong coupling effect of KH570, it forms a dense gel coating with SiO_2 sol. Moreover, KH570 and SiO_2 sol can adhere to cotton fibers via hydrogen bonds, which effectively conceal the spacing and orientation of the fibers. The surface

morphology of AMP- SiO_2 -KH570@COT is nearly identical to that of SiO_2 -KH570@COT, but the cracking phenomenon is improved. This is likely due to the double-layer coating, which alleviates the cracking caused by high temperatures during the curing process.

Furthermore, the elemental content and distribution of AMP- SiO_2 -KH570@COT are further investigated by EDX (Fig. 4), and element mapping (Fig. 5). It is evident that the raw fabric consists solely of C and O elements, whereas AMP- SiO_2 -KH570@COT contains significant amounts of C, O, and Si elements, which originate from both the raw fabric and the incorporated SiO_2 sol. Additionally, the presence and uniform distribution of small amounts of P and N elements suggest that AMP has been evenly applied to the cotton fabric through the first layer of AMP sol. However, due to the limited addition of AMP and its positioning within the inner layer of the double-layer sol, the elemental contents detected by the mapping probe are relatively low. These results and observations are consistent with findings reported in other related studies^[27,29,30].

Surface elemental analysis

Figure 6 illustrates the distribution of surface elements in both raw and sol-finished fabrics.

For raw cotton fabric, characteristic peaks for two elements are observed: one at 284.5 eV corresponding to C_{1s} and another at 532.2 eV corresponding to O_{1s} . These peaks indicate that the cotton fiber is primarily composed of cellulose, with carbon and oxygen as the major elements (as shown in Fig. 4a). For SiO_2 @COT, in addition to the aforementioned peaks, new characteristic peaks appear at 102.4 and 154.0 eV, corresponding to Si_{2p} and Si_{2s} , respectively. These peaks confirm that silicon atoms are incorporated into the fabric structure, further supporting the conclusion that SiO_2 sol effectively coats the fiber surface. For AMP@COT, N_{1s} and P_{2p} absorption peaks are observed around 398.6 and 135.3 eV, which correspond to the N element of the nitrogen-containing base and the P element of the phosphate group in AMP. However, due to the small amount of AMP used as a flame retardant, these two peaks are not very prominent. In addition, a slight decrease in the C_{1s} binding energy value is observed for the AMP- SiO_2 -KH570@COT compared to SiO_2 -KH570@COT. This suggests that KH570 has a coupling effect, forming a chemical bond between SiO_2 sol and KH570. The addition of AMP slightly disrupts the irregular spatial arrangement of KH570. Meanwhile, the treated fabric surface shows N_{1s} and P_{2p} absorption

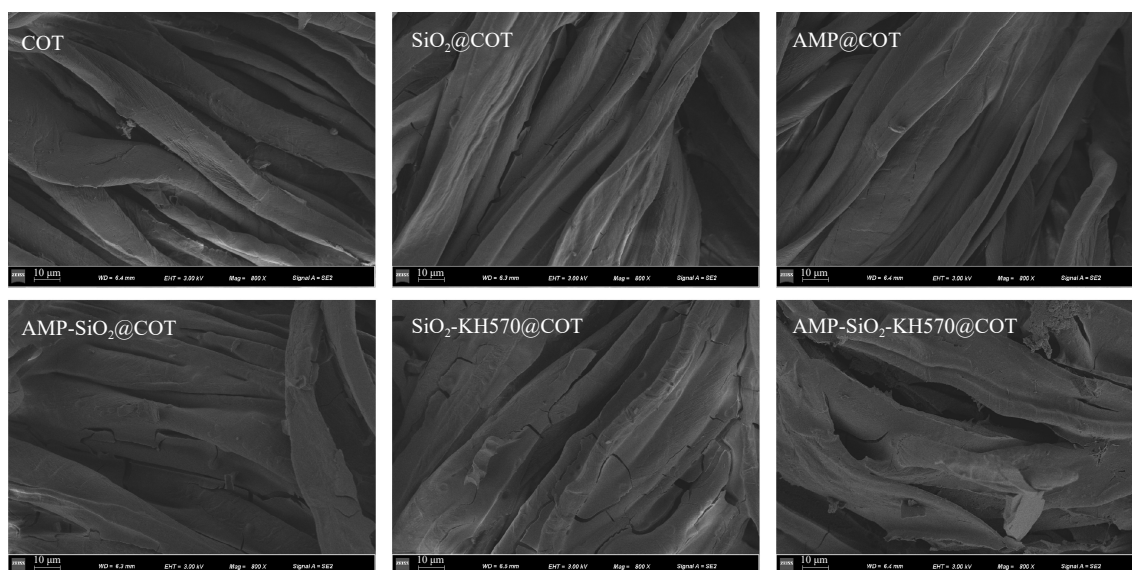


Fig. 3 SEM images of raw and treated cotton fabrics.

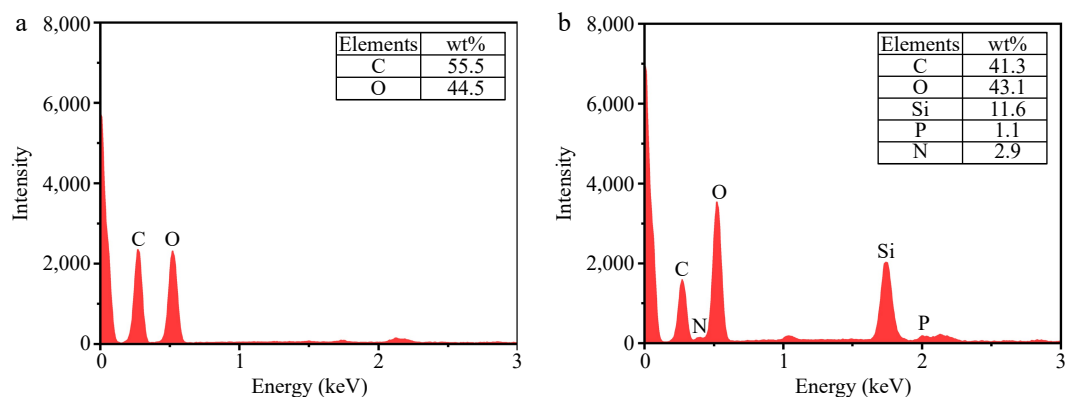


Fig. 4 (a) EDX spectra of COT, and (b) AMP-SiO₂-KH570@COT.

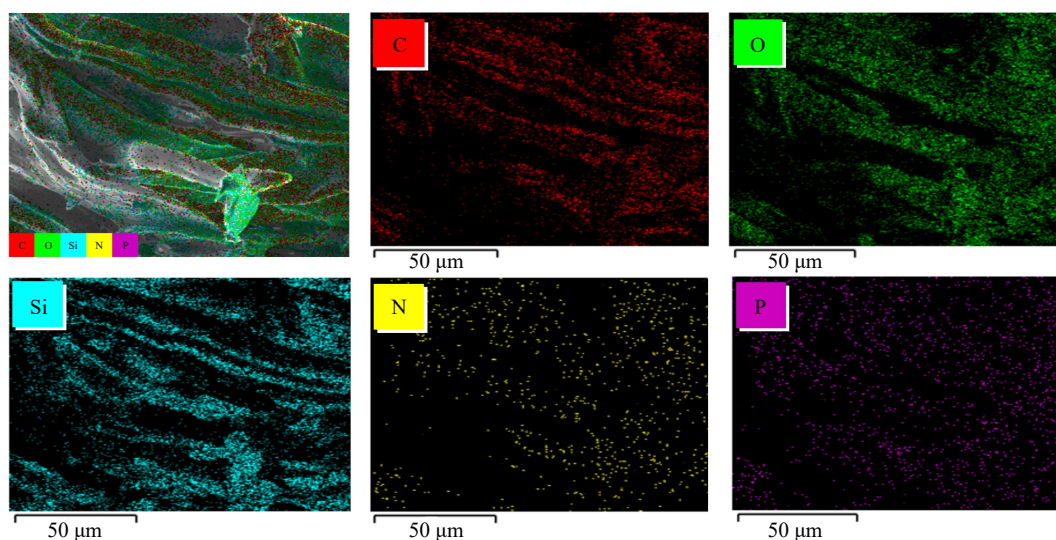


Fig. 5 Elements distribution images of AMP-SiO₂-KH570@COT (depicting the mapping of carbon (C), oxygen (O), silicon (Si), nitrogen (N), and phosphorus (P) elements).

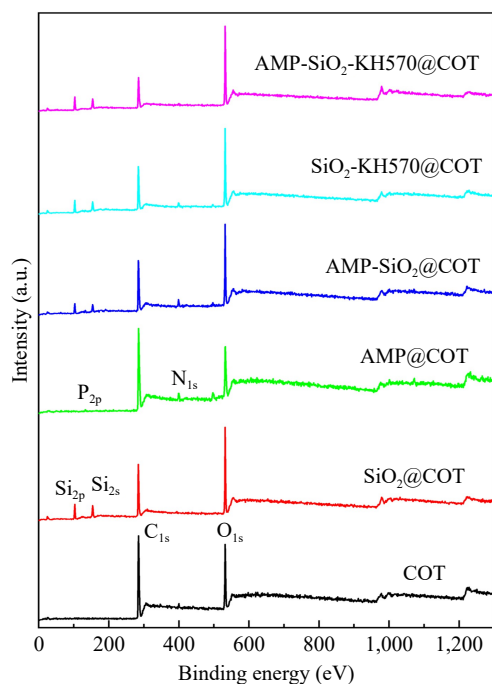


Fig. 6 XPS spectra of raw and treated cotton fabrics.

peaks, and their distribution is relatively uniform, consistent with the results observed by the mapping probe.

The high-resolution XPS spectrum of AMP-SiO₂-KH570@COT is shown in Fig. 7. In the deconvolution of O_{1s}, three characteristic peaks are observed at 532.6 eV, 532.1 eV, and 531.9 eV, corresponding to C-O-C/C-OH/C-O-P, P=O/C=O, and Si-O-C/Si-O-Si bonds^[31,32], respectively. Specifically, the C-O-C and C-OH peaks primarily originate from the cellulose backbone, while the C-O-P and P=O peaks are derived from the pentose sugar and phosphate groups in AMP. The C=O peak is associated with the silane coupling agent KH570. The detection of Si-O-Si bonds confirms the successful attachment of SiO₂ sol to the cotton fabric surface, forming a unique three-dimensional network structure with Si-O-Si as the backbone. This further confirms the successful attachment of the double-layer sol to the fabric surface. In the Si_{2p} spectrum, three peaks of Si-C (102.2 eV), Si-O-C (102.9 eV), and Si-O-Si (103.6 eV) are observed, corresponding to the Si-O-Si structure formed by KH570 and SiO₂, thereby confirming the successful modification of SiO₂ by KH570. These results suggest that KH570 not only serves as a coupling agent but also plays a significant role in the formation of Si-O-Si bonds, which are critical for the structural stability and effectiveness of the flame-retardant system.

Internal chemical composition analysis

Figure 8 shows FTIR spectra of raw and sol-finished fabrics. The primary characteristic peaks are observed for the raw fabric at

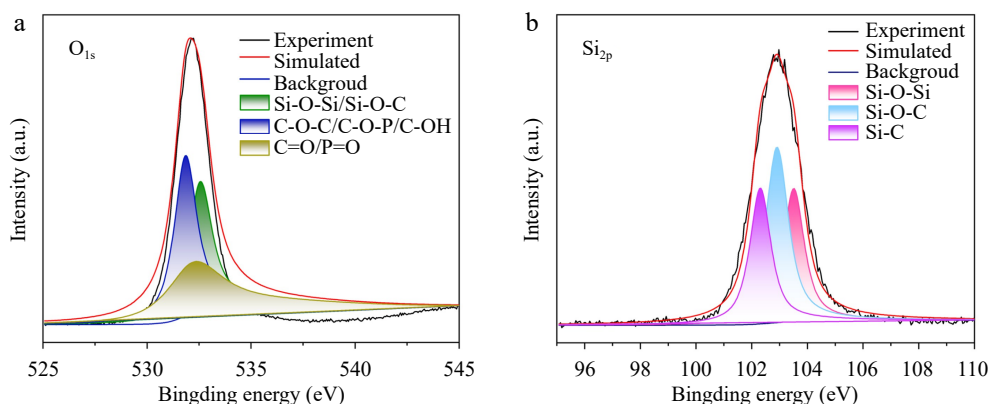


Fig. 7 High resolution XPS spectra for (a) O_{1s} , and (b) Si_{2p} of AMP- SiO_2 -KH570@COT.

$3,410\text{ cm}^{-1}$ (-OH stretching vibration), $2,915\text{ cm}^{-1}$ ($-CH_2$ stretching vibration), $1,426\text{ cm}^{-1}$ (C-H in-plane bending), $1,313\text{ cm}^{-1}$ (C-H stretching vibration), and $1,026\text{ cm}^{-1}$ (C-O-C stretching vibration of the cellulose backbone)^[15,33]. Additionally, a distinct peak at $1,626\text{ cm}^{-1}$ (C=C) suggests that the system undergoes a dehydration process, leading to the formation of aldehydes, ketones, and other olefinic compounds^[34]. Following the series sol coating treatment, the aforementioned functional groups remain present, indicating that the raw molecular structure of the cotton fabric is not altered. Furthermore, the FTIR spectra of the sol-finished cotton fabrics exhibit new absorption peaks. For SiO_2 @COT, a new absorption peak is observed in the range of $1,150\text{--}1,060\text{ cm}^{-1}$, attributed to the Si-O stretching vibration. This peak is not only derived from the internal structure of the SiO_2 sol but also indicates that a crosslinked structure is formed through the -OH groups exposed on the fabric backbone and those exposed within the SiO_2 sol. These findings are consistent with the results obtained from EDX and XPS analyses.

For AMP@COT, the peaks are observed at $1,250$ and $1,110\text{ cm}^{-1}$, corresponding to P=O and P-O-C bonds in AMP, respectively. The broad infrared absorption at $3,195\text{ cm}^{-1}$ originates from the stretching vibration of NH groups, while the peak at $1,654\text{ cm}^{-1}$ is assigned

to the C-N ring vibration of adenine^[35]. In contrast to AMP@COT, SiO_2 -AMP@COT exhibits a new characteristic peak at approximately 802 cm^{-1} , which results from the vibrational overlap of Si-O-Si and P-O-C bonds. This suggests that the phosphate group in AMP has formed a hydrogen bond with the -OH groups on the exterior of the SiO_2 molecule, which is then linked to the -OH groups on the cotton fabric surface. For SiO_2 -KH570@COT, characteristic peaks of Si-O-C and C=O are observed at $1,050$ and $1,720\text{ cm}^{-1}$, respectively. Additionally, the intensities of the -OH and Si-OH peaks are notably reduced, which can be attributed to the presence of SiO_2 , the condensation reaction of KH570, and the molecular structure of KH570, is shown in Fig. 1a. The peaks at $3,550\text{--}3,200\text{ cm}^{-1}$ of AMP- SiO_2 @COT, SiO_2 -KH570@COT, and AMP- SiO_2 -KH570@COT are broadened, which is due to the effect of hydrogen bonding, indicating that the AMP and SiO_2 molecules are connected via hydrogen bonds, as shown in Fig. 1b. In comparison to the untreated cotton fabrics, the C-C stretching vibrations of the treated cotton fabrics shifted to higher frequencies. This shift is attributed to the chemical chain growth induced by the interaction between the flame retardant and cellulose, which increases the exo-chain bond angle of the C-C bond. Additionally, the modified silane groups bind to the cellulose's hydroxyl sites, leading to greater distortion in the cellulose network^[36].

Crystal structure analysis

Figure 9 presents the XRD patterns of raw and sol-finished fabrics. The XRD spectra of raw and treated cotton fabrics exhibit remarkable similarity, suggesting that the crystal structure of cotton fibers remains largely intact and is not significantly altered by the SiO_2 , KH570, and AMP treatments. Cellulose chains in the raw cotton fabric exhibit a specific crystalline structure, forming a typical crystalline arrangement. Diffraction peaks corresponding to the cellulose crystals appear at 14.9° , 16.5° , 22.9° , and 34.3° ^[37], respectively. In comparison, cotton fabric that has undergone treatment shows a certain degree of sol coverage and chemical cross-linking, which leads to a noticeable reduction in the intensity of these diffraction peaks.

For SiO_2 @COT, its diffraction pattern is nearly identical to that of the raw cotton fabric. It is primarily because the diffraction peak at 22.9° corresponding to cotton has a prominent intensity, while the diffraction peak of SiO_2 (about 22.0°) is relatively weak. High intensity peaks mask the role of weak peaks. The XRD patterns of the AMP@COT and AMP- SiO_2 @COT do not change significantly, indicating that AMP is likely to be amorphous and lack an ordered crystal structure. Most of cotton fabrics and flame retardants are connected by hydrogen bonds, and the crystal structure will hardly change. If it changes, it may be a slight change in the peak position or peak

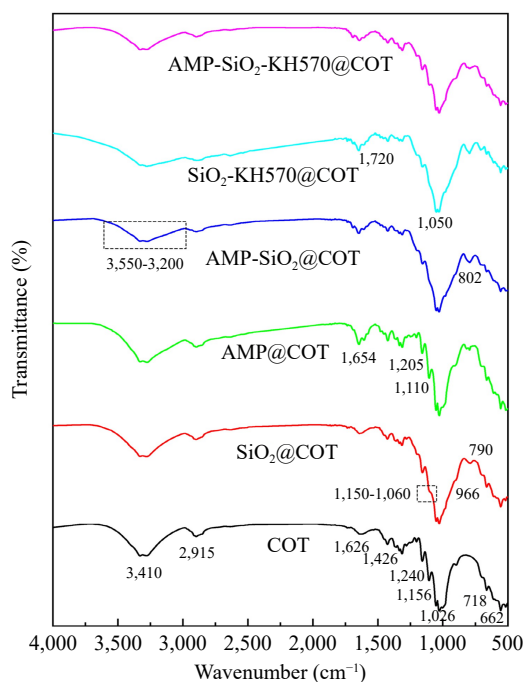


Fig. 8 FTIR spectra of raw and treated cotton fabrics.

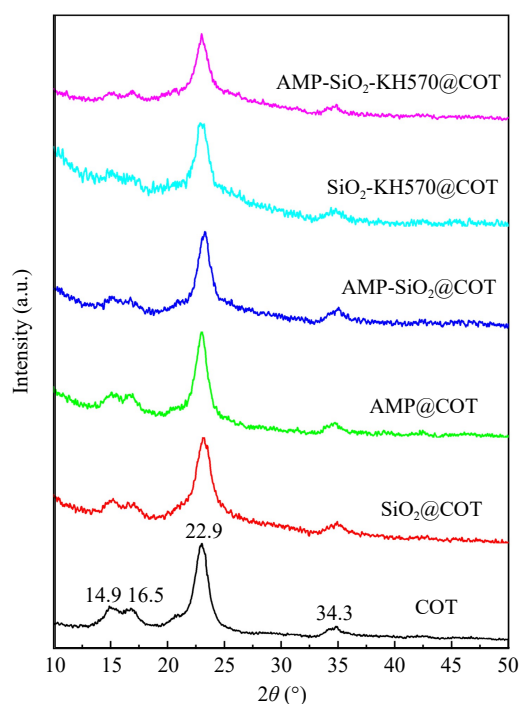


Fig. 9 XRD patterns of raw and treated cotton fabrics.

intensity level, but no new phase (new peak position) will be generated. It can be found from Fig. 9 that the diffraction peaks at 14.9° and 16.5° of the KH570-modified fabric are diminished. This weakening suggests that the hydrogen bond interactions between the modified groups result in an expansion of the crystal lattice of the cotton fabric, allowing some KH570 molecules to penetrate the internal channels.

Thermal stability analysis

Figure 10 shows the TG and derivative thermogravimetric (DTG) curves of the fabrics under an N₂ atmosphere, with the main pyrolysis data provided in Table 2. The relevant data include: the temperature at 10 wt% mass loss ($T_{10\%}$), the temperature of maximum mass loss rate (T_{max}), the maximum mass loss rate (R_{max}), and the char residue rate at 700.0 °C. The weight gain rate (WGR) of the treated cotton fabrics can be determined using formula (1):

$$WGR = \frac{W_f - W_i}{W_i} \times 100\% \quad (1)$$

where, W_i : the weight of the cotton fabric before impregnation; W_f : the weight of the cotton fabric after impregnation.

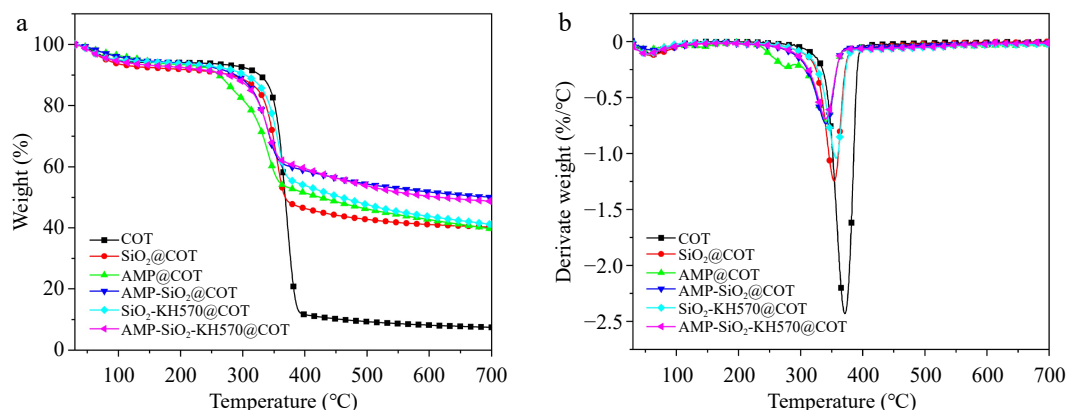


Fig. 10 (a) TG, and (b) DTG curves of raw and treated cotton fabrics (10 K/min, N₂).

For raw cotton fabric, three distinct stages of pyrolysis are clearly observed. Before 100.0 °C, a slight weight loss is observed, attributed to the evaporation of free and bound water in the cotton fibers under heating. The range of 302.5 and 393.4 °C is the main pyrolysis stage, with approximately 80.4% mass loss. During this phase, cellulose undergoes glycosylation reactions, decomposing into levoglucosan, which further breaks down into small solid carbon residues and combustible gases. Afterward, the decomposition, and carbonization take place. As the temperature continues to rise, the intermediate pyrolysis products and formed char are further decomposed, and only 7.5% char residue is retained at 700.0 °C.

As shown in Fig. 10 and Table 2, the treated fabrics exhibit earlier pyrolysis compared to the raw cotton fabric. For SiO₂@COT, its $T_{10\%}$ (284.3 °C) and T_{max} (353.3 °C) values are lower by 13.2% and 4.8% than raw fabric, and the char residue rate (40.3%) dramatically increases by 437.3%. This significant increase is mainly due to the water released from the SiO₂ sol coating, which absorbs substantial heat, reduces the combustion surface temperature, and dilutes the concentration of intermediate pyrolysis products. Additionally, the high melting point of SiO₂ sol provides structural support for the char residue. With the continuous increase of the pyrolysis temperature, the SiO₂ coating is pre-pyrolyzed and cracked. After the protection is lost, the cotton fabric is heated and begins the second round of pyrolysis and carbonization. Whereas for SiO₂-KH570@COT, its pyrolysis is not advanced, and its R_{max} (1.0 %/°C) is slightly lower than that of SiO₂@COT. This may be due to the chemical chain growth after the introduction of KH570 into the SiO₂ network, and the chemical bond-breaking requires more heat to be absorbed. For AMP@COT, its $T_{10\%}$ and T_{max} are relatively lower. This is likely due to the decomposition of the phosphoric acid group in AMP at a lower temperature (about 215.0 °C), which releases phosphoric acid. This, in turn, accelerates the loss of water from cellulose and facilitates the creation of aromatic char. Furthermore, the synergistic effect of P-N enhances the formation of heat-resistant aromatic compounds[38]. Studies have demonstrated that N in P-N flame retardants facilitates interactions with phosphate groups, which increases the polarity of the P-N bond and enhances the electrophilicity of the phosphorus atom, thereby promoting the carbonization of fibers. Additionally, nitrogen-containing bases decompose under heat to produce substances that act as effective flame retardants, such as aromatic diazonium salts and azo compounds[39]. Due to the catalytic effect of AMP, a further advancement of $T_{10\%}$ and T_{max} is also observed in the AMP-SiO₂@COT, which exhibits the highest amount of char residue rate. This likely benefits from the physical adsorption and hydrogen bonding interactions between AMP molecules and SiO₂.

Table 2. Main pyrolysis data of raw and treated cotton fabrics.

Sample	WGR (%)	T _{10%} (°C)	T _{max} (°C)	R _{max} (%/°C)	Char residue rate (%)
COT	—	327.5	371.2	2.4	7.5
SiO ₂ @COT	28.3	284.3	353.3	1.3	40.3
AMP@COT	35.0	262.1	339.6	0.7	39.7
AMP-SiO ₂ @COT	54.4	288.2	340.7	0.7	49.8
SiO ₂ -KH570@COT	83.8	304.7	357.2	1.0	41.1
AMP-SiO ₂ -KH570@COT	89.5	277.2	340.6	0.6	49.1

Through the synergistic effect of SiO₂, AMP, and KH570, AMP-SiO₂-KH570@COT achieves the optimal R_{max} (0.6 %/°C) and char residue rate (49.1%), which indicates that the Si-O-Si structure provides high thermal stability, acting as an effective barrier to block flame and oxygen. Additionally, the phosphoric acid group in AMP contributes to char layer formation by decomposing at high temperatures and promoting cellulose dehydration, indicating that KH570 optimizes the structure of SiO₂. Interestingly, despite the similar coating content in AMP-SiO₂-KH570@COT and SiO₂-KH570@COT, the former shows better thermal stability. This suggests that AMP and SiO₂-KH570 synergistically enhance the heat resistance of cotton fabrics.

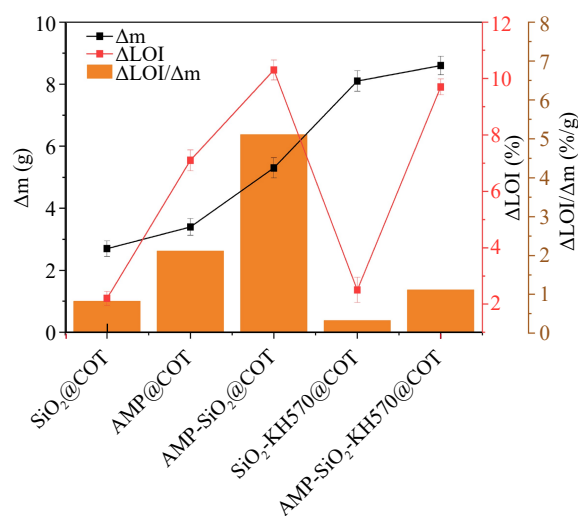
Flammability analysis

The flame retardancy of the fabrics is assessed using LOI and VFT, with the data shown in Table 3. The variations in Δm, ΔLOI, and the ratio ΔLOI/Δm for cotton fabrics before and after treatment are depicted in Fig. 11. Additionally, Fig. 12 shows the VFT results of the cotton fabrics before and after series sol-finishing. Δm represents the mass change of the treated cotton fabric after dipping and drying, ΔLOI/Δm represents the increment in LOI per unit mass increase^[29]. T₁ is the after-flame time, T₂ is the after-glow time, and CL is the damaged length. LOI is commonly used to categorize the flame retardant properties^[40]: 0.0%~22.0% are inflammable materials; 22.0%~27.0% are combustible materials; more than 27.0% are non-flammable materials.

As shown in Table 3, for SiO₂@COT, the increase in LOI indicates that the SiO₂ gel, deposited on the cotton fabric through hydrogen bonding, effectively blocks external penetration of oxygen and heat. This deposition also restricts the exchange of gaseous products and heat from the interior, thereby delaying the decomposition of the cotton fibers. These observations are in line with the earlier analysis. For AMP@COT, the LOI (25.1%) reaches the combustible level, which can be attributed to the smaller molecular size of AMP, allowing it to adsorb more readily onto the cotton fabric surface. Moreover, the synergistic effect of phosphoric acid and P-N compounds generated during the decomposition of AMP promotes the formation of aromatic structures, which help to isolate heat and combustible gases, thereby improving flame resistance^[41]. For AMP-SiO₂@COT, the LOI reaches 28.3%, shifting its flame retardant grade changes from inflammable to non-flammable. The double-layer sol coating not only provides more effective flame retardant components (Δm = 5.3 g) to the cotton fabric but also enables SiO₂ and AMP to

work synergistically, demonstrating a certain degree of synergy. Notably, the ΔLOI/Δm of AMP-SiO₂@COT reaches as high as 5.1 %/g, highlighting the enhanced flame retardant effect of P and N in AMP on SiO₂. However, the addition of KH570 does not significantly increase the LOI, despite the observed increase in weight gain. This suggests that KH570 itself does not contribute directly to the flame retardant effect but primarily functions to modify the SiO₂ structure.

The above results are further supported by VFT. Rapid combustion is observed for the raw cotton fabric (T₁ = 7.5 s), followed by a smoldering phase (T₂ = 15.0 s) after ignition, resulting in minimal char residue (Fig. 12a). For SiO₂@COT, its T₁ is 23.0 s and T₂ is 0.7 s. This indicates a more substantial char residue, suggesting that the SiO₂ coating provides some protection to the cellulose by slowing the spread of the flame. However, the protective layer formed by silica sol cannot prevent cellulose from burning and achieve self-extinguishing, as its flame-retardant performance is constrained. For AMP@COT, T₁ (3.8 s) decreases by 83.5%, and T₂ reaches 0 s compared with SiO₂@COT, showing its excellent self-extinguishing property and the fabric damage length is 14.6 cm, which indicates that AMP decomposes phosphoric acid by pyrolysis and induces cellulose formation of more coke and volatiles. At the same time, the T₁ of AMP-SiO₂@COT is reduced to 3 s, and then the burning is stopped, which fully reflects the synergistic effect of AMP and SiO₂. SiO₂-KH570@COT exhibits a shorter T₂ and a higher char residue compared to the raw fabric (Fig. 12e). This indicates that KH570 endows SiO₂ with a structure that is more resistant to high temperature and flame to a certain extent. AMP-SiO₂-KH570@COT exhibits self-extinguishing properties, with a damage length of only 8.2 cm. These findings confirm our previous speculation that AMP-SiO₂-KH570 can effectively promote cellulolysis, resulting in the development of a stable char structure. Now it should be known that the enhanced thermal stability of the treated cotton fabrics, as

**Fig. 11** Δm, ΔLOI, and the ratio ΔLOI/Δm of raw and treated cotton fabrics.**Table 3.** LOI and VFT data of raw and treated cotton fabrics.

Sample	LOI (%)	ΔLOI (%)	Δm (g)	ΔLOI/Δm (%/g)	Flammability level	T ₁ (s)	T ₂ (s)	CL (cm)
COT	18.0	—	—	—	Inflammable	7.5	15.0	30.0
SiO ₂ @COT	20.2	2.2	2.7	0.8	Inflammable	23.0	0.7	30.0
AMP@COT	25.1	7.1	3.4	2.1	Combustible	3.8	0	14.6
AMP-SiO ₂ @COT	28.3	10.3	5.3	5.1	Non-flammable	3.0	0	8.9
SiO ₂ -KH570@COT	20.5	2.5	8.1	0.3	Inflammable	14.7	1.2	30.0
AMP-SiO ₂ -KH570@COT	27.7	9.7	8.6	1.1	Non-flammable	2.2	0	8.2

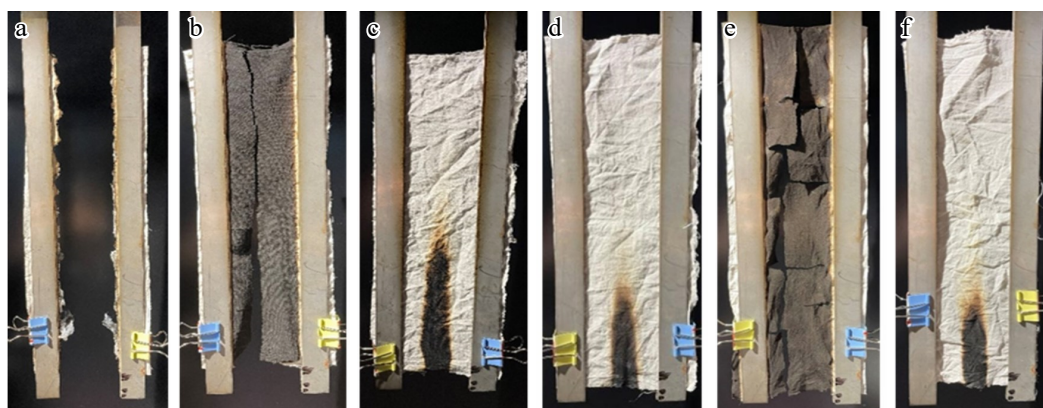


Fig. 12 VFT results of (a) COT, (b) SiO_2 @COT, (c) AMP@COT, (d) AMP- SiO_2 @COT, (e) SiO_2 -KH570@COT, (f) AMP- SiO_2 -KH570@COT.

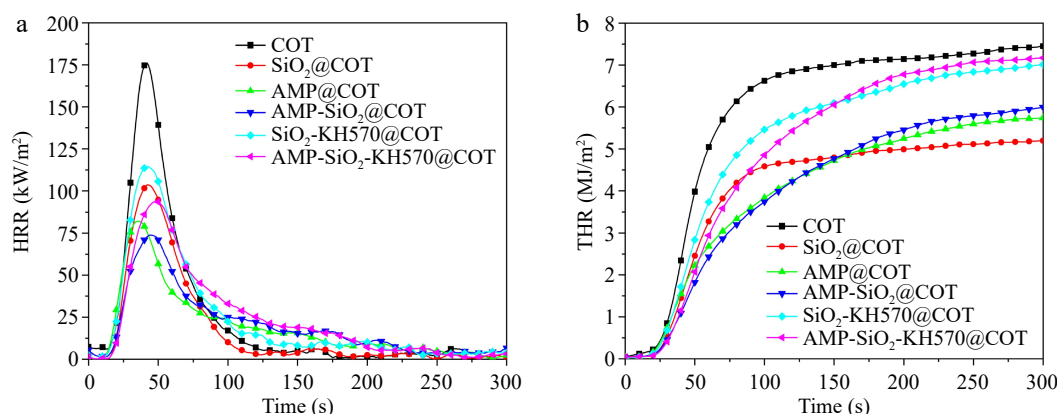


Fig. 13 Relationship between (a) HRR, (b) THR, and time for raw and treated cotton fabrics.

indicated by the TG and DTG curves, directly contribute to their improved flame retardancy. The higher char residue rate at high temperatures provides a physical barrier, reducing heat, oxygen, and fuel transfer, which is consistent with the results of the LOI and VFT tests. The synergistic interaction between the P-N, and Si components effectively inhibits the continued combustion of the cotton fabric^[42]. The cotton fabric treated with AMP demonstrates superior fire retardancy and self-extinguishing capabilities, coupled with the dual protective mechanism of AMP sol and SiO_2 sol, presenting a promising approach for creating advanced, high-performance materials with enhanced fire protection.

Combustion property analysis

The combustion performance of the fabrics is evaluated using CCT, with the results presented in Fig. 13 and Table 4. The specific parameters measured included time to ignition (TTI), peak heat release rate (PHRR), time to reach PHRR (TPHRR), total heat release (THR), and fire growth rate index (FGR). The graph in Fig. 14 shows the performance of treated fabrics under CCT.

The raw cotton fabric exhibits rapid combustion, with PHRR reaching 183.1 kW/m^2 and THR at 7.5 MJ/m^2 , further indicating its low flame retardancy. For SiO_2 @COT, its PHRR, and THR are reduced to 104.2 kW/m^2 and 5.2 MJ/m^2 , respectively, demonstrating that the SiO_2 sol coating significantly enhances the fabric's flame resistance. However, for SiO_2 -KH570@COT, its PHRR and THR do not decrease, but increase slightly, which also verifies that KH570 does not possess flame retardancy. When AMP sol treats the cotton fabric, its PHRR is reduced by 20.6 kW/m^2 compared to SiO_2 @COT, the TTI occurs 6 s earlier, and the THR trend remains the same. Therefore, AMP demonstrates remarkable catalytic ability in char formation

and smoke suppression, accelerating the reaction process and significantly enhancing the flame resistance of cotton fabrics.

Relative to other samples, AMP- SiO_2 @COT exhibited the lowest PHRR at 75.2 kW/m^2 , which benefits from the AMP's ability to form char and the barrier effect of SiO_2 , and also reflects the outstanding synergistic effect of AMP- SiO_2 . This combination results in enhanced flame resistance. Moreover, the FGR of AMP- SiO_2 @COT and AMP- SiO_2 -KH570@COT decreases by 60.0% and 56.9%, respectively, relative to the raw fabric. The TPHRR of both AMP- SiO_2 @COT and AMP- SiO_2 -KH570@COT are delayed by 1 and 7 s, respectively, in comparison to the raw cotton fabric. This indicates that both treatments can effectively delay the onset of a fire, with AMP- SiO_2 -KH570@COT exhibiting a more pronounced retardation effect. These results suggest that the ternary composite system of AMP, SiO_2 , and KH570 provides superior flame resistance and combustion delay compared to the binary AMP- SiO_2 system alone.

Figure 14 shows a graph of treated fabrics subjected to CCT. As shown in Fig. 14a, the raw cotton fabric leaves almost no char residue, which aligns with the results observed for VFT. For

Table 4. CCT data of raw and treated cotton fabrics.

Sample	TTI (s)	PHRR (kW/m^2)	TPHRR (s)	THR (MJ/m^2)	FGR ($\text{kW}/(\text{m}^2\text{s})$)
COT	7.0	183.1	36.0	7.5	5.1
SiO_2 @COT	8.0	104.2	36.0	5.2	2.9
AMP@COT	6.0	83.6	30.0	5.7	2.8
AMP- SiO_2 @COT	8.0	75.2	37.0	6.0	2.0
SiO_2 -KH570@COT	7.0	115.4	36.0	7.0	3.2
AMP- SiO_2 -KH570@COT	8.0	94.3	43.0	7.2	2.2



Fig. 14 CCT photos of raw and treated cotton fabrics. (a) COT, (b) SiO_2 @COT, (c) AMP@COT, (d) AMP- SiO_2 @COT, (e) SiO_2 -KH570@COT, (f) AMP- SiO_2 -KH570@COT.

SiO_2 @COT, only a limited char residue is observed, with a large area of white material visible at the center of the char layer. This is derived from the silica and Si-C compounds formed by the decomposition of SiO_2 sol under high-temperature flame exposure, providing protection to the inner fibers by blocking heat and gas. The cotton fabrics treated with AMP single-layer sol and AMP- SiO_2 double-layer sol formed continuous and compact char layers on their surfaces. The char layers expanded by 2.5 cm for AMP single-layer sol and 2 cm for AMP- SiO_2 double-layer sol, due to the expansion and foaming caused by the nitrogen-containing bases in the AMP structure. Combined with Fig. 3, the surface of the silica sol modified by KH570 has a cracking phenomenon, which weakens its flame retardant effect, and in Fig. 14e, the surface of the char residue appears yellowing. However, Fig. 14f reveals the char structure of AMP- SiO_2 -KH570@COT is more obvious and denser than that of AMP- SiO_2 @COT, with the swelling height reaching 3 cm. This

demonstrates the outstanding flame-retardant effect of AMP- SiO_2 -KH570@COT. Therefore, the development of a well-formed expanded, and dense char layer is a key factor contributing to the enhanced fire resistance of cotton fabrics.

Char residue analysis

Figure 15 displays the SEM images of residues of the char. The char residue of the raw cotton fabric resembles a floating floc, loose, and small. For SiO_2 @COT, from Fig. 3, its morphology can be seen to be continuous, dense, and complete before burning. Although it shows fracture and shedding characteristics after burning, the fiber structure wrapped in it is mostly intact and has a clear twisted structure and trend. This finding confirms our inference on the combustion mode, process, and mechanism of silica sol-treated cotton fabrics. During the early stage of combustion, silica functions as a protective barrier, effectively preventing heat and oxygen from reaching the cotton fibers, thereby demonstrating significant flame

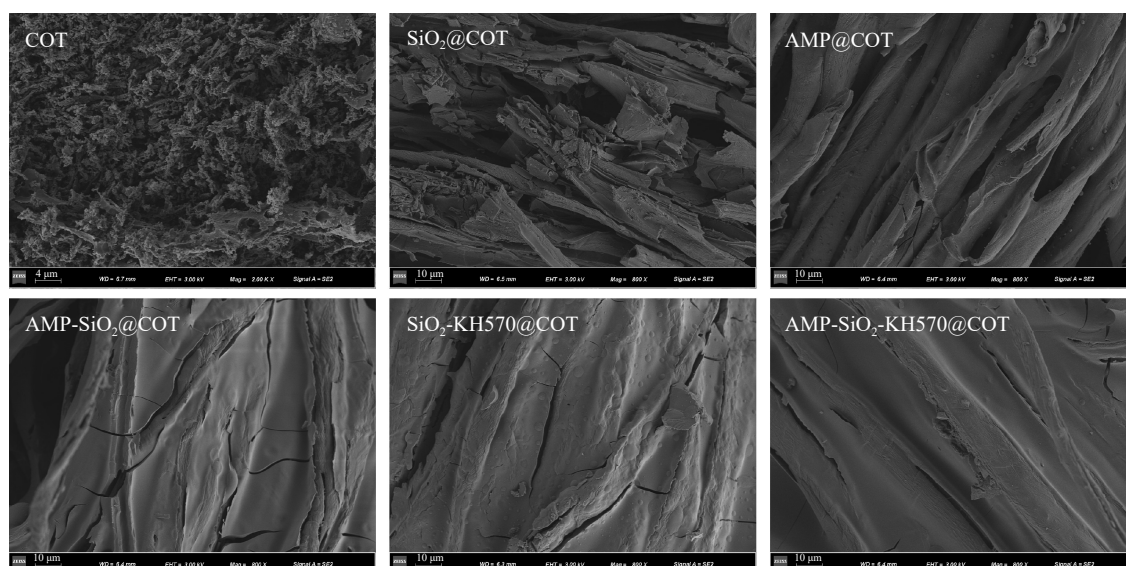


Fig. 15 SEM images of char residues after VFT.

resistance. Compared with raw cotton, the twisted ribbon morphology of AMP@COT is clearly defined, and the char layer is relatively complete. This can be ascribed to the synergistic effects of nitrogen-containing and phosphate components of AMP. SiO_2 -AMP@COT not only combines the advantages of SiO_2 sol and AMP, but also features an intact surface protective layer, resulting in exceptionally high char residues and improved flame retardant efficiency. However, it exhibits cracks, and its surface is not entirely smooth. Except for a few cracks caused by gel rupture, the surface of SiO_2 -KH570@COT remains intact, demonstrating stable fire resistance. The surface gel layer of AMP- SiO_2 -KH570@COT is smooth and complete, without any visible cracks. This results from the synergistic effects of SiO_2 and AMP, along with the coupling effect of KH570 and hydrogen bonding, which collectively enhance the overall flame retardant performance. Furthermore, the porous layer generated after combustion on the AMP- SiO_2 -KH570@COT surface can effectively isolate the transfer between the outer layer and cotton fibers, thereby cutting off the combustion elements.

Analysis of flame retardant mechanism

The flame retardant mechanism of SiO_2 -AMP-KH570@COT is shown in Fig. 16, based on the analysis presented above. Cellulose is the main component of cotton fabric, accounting for about 94 %. It contains a lot of hydroxyl groups. When it encounters a fire source and burns, it decomposes and serves as a carbon source during combustion.

As shown in Fig. 16, during the thermal cracking process, cellulose undergoes dehydration and carbonization, resulting in the production of water vapor, carbon dioxide, a large amount of heat, and residues^[43]. The SiO_2 gel coating is adsorbed mainly by physical attachment and chemical hydrogen bonding. It is further converted into graphite or glassy carbon, forming a dense protective layer and creating a barrier effect at high temperatures, effectively isolating oxygen and heat^[30,44]. The coupling effect of KH570 and hydrogen bonding force creates a structural framework and links each component, thereby enhancing the overall flame-retardant performance.

The modification of SiO_2 sol with KH570 results in treated cotton fabric that retains its surface crystalline structure, while the modification reaction occurs in the non-crystalline regions of the fiber surface, facilitated by specific folding. At the same time, the interaction between the double-layer sol and the AMP sol results in an enhanced performance. AMP molecules are closely connected with SiO_2 sol particles and cotton fabrics through physical adsorption and hydrogen bonding forces. They play an important interaction and synergistic flame retardant effect. When the AMP sol coating is

heated, phosphoric acid can be released, promoting the development of aromatic char structures by removing water from the cotton fibers, advancing the pyrolysis reactions, and endowing cotton fabrics with higher LOI values and stronger self-extinguishing abilities. In addition, the phosphate groups in AMP catalyzes carbon formation and inhibit heat release. Overall, the pyrolytic foaming effect of nitrogen-containing substrate and the physical barrier effect provided by the silica sol play a good synergistic effect.

Conclusions

In this study, a ternary sol-gel system is prepared using the sol-gel technique and dipping-drying method, which is then applied to the surface of cotton fabric. The particle size of KH570-modified SiO_2 sol reaches the micron level, exhibiting a unique Si-O-Si three-dimensional skeleton structure. This structure helps maintain the stability of the crystal form on the surface of the treated cotton fabric. The pyrolysis reaction of the cotton fabric after finishing is advanced, with the dense SiO_2 gel coating forming a protective barrier in a high-temperature environments, effectively isolating heat and oxygen. Additionally, AMP gel releases phosphoric acid upon the pyrolysis of phosphoric acid groups at high temperatures, promoting the formation of coke. Once the nitrogen-containing substrate undergoes pyrolysis, the system foams and expands, further isolating heat and oxygen. When these components act together, both the PHRR and THR are effectively reduced, demonstrating excellent synergistic flame retardant performances.

As a result, the LOI of the double-layer sol-finished cotton fabric (AMP- SiO_2 @COT) reaches 28.3%, which is 10.3% higher than that of the untreated fabric. The fabric treated with AMP- SiO_2 -KH570 shows the second highest LOI (27.7%), the shortest char length (8.2 cm), the highest char residue rate (48.7%) and the most favorable times for ($T_1 = 2.2$ s) and ($T_2 = 0$ s). Furthermore, in a CCT, the AMP- SiO_2 -KH570@COT shows the second-lowest THR (7.2 MJ/m²). Compared with the raw cotton fabric, the residual carbon content increases by 551.2%, the PHRR (94.3 kW/m²) decreases by 48.5%, and the TPHRR (43.0 s) is delayed by 7 s. While the introduction of KH570-modified SiO_2 may slightly weaken the synergistic effect of SiO_2 and AMP, the corresponding LOI value and residual char content are not as favorable as those of the double-layer sol-treated fabric. Nevertheless, as a new bio-based flame retardant, AMP offers a promising option for the development of eco-friendly flame retardant functional materials. In future studies, alternative ratios, coupling agents, or even entire ternary systems are valuable to be explored. However, the current study has some limitations. The long-term durability of the

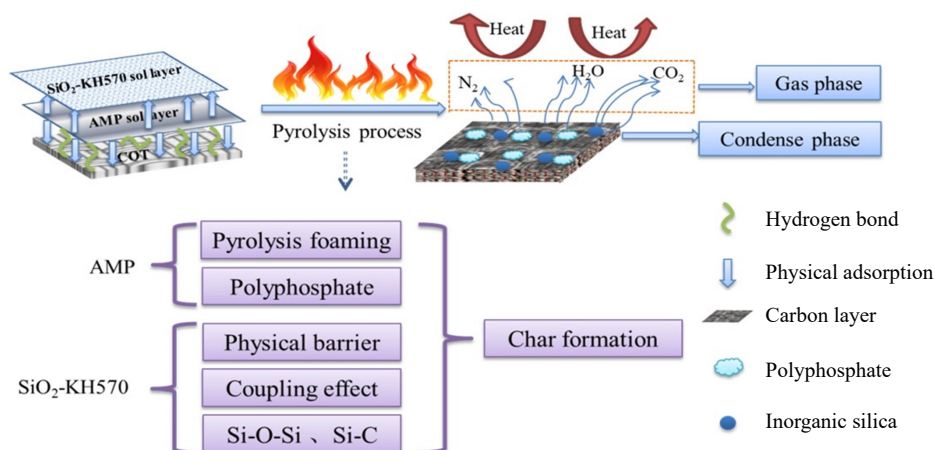


Fig. 16 The flame retardancy mechanism of AMP- SiO_2 -KH570@COT.

flame retardant gel coatings under different environmental conditions was not investigated. Future studies could focus on: (1) evaluating the stability of the coatings over time and exploring ways to improve their durability; (2) exploring alternative ratios of AMP, SiO₂, and KH570; and (3) investigating the performances of other coupling agents in the system.

Author contributions

The authors confirm contribution to the paper as follows: overall conception and design of the research: You F, Liu M; provision of resources (including experimental materials, research funds, equipment and facilities, etc.): You F; data collection, processing and paper writing: Liu M; review of the results, revision and approval of the final version of the manuscript: You F, Lu Q, Wang Z, Zhang Y, Huang H. All authors reviewed the results and approved the final version of the manuscript.

Data availability

All data generated or analyzed during this study are included in this published article.

Acknowledgments

The study is financially supported by the National Natural Science Foundation of China (Grant Nos 51376089 and 50906039), and the Natural Science Foundation of Jiangsu Province (Grant No. BK20230318). Li D is specially thanked for her valuable experimental preparations of this study.

Conflict of interest

The authors declare that they have no conflict of interest.

Dates

Received 10 November 2024; Revised 11 January 2025; Accepted 20 January 2025; Published online 24 February 2025

References

- Li S, Huang S, Xu F, Zhao T, Zhang F, et al. 2020. Imparting superhydrophobicity and flame retardancy simultaneously on cotton fabrics. *Cellulose* 27(7):3989–4005
- Chen C, Luan J, Lan F, Ji G, Yin X, et al. 2024. Construction and application of B/P/N durable flame retardant crosslinking system on cotton fabric. *Industrial Crops and Products* 222:119623
- Qin H, Li X, Zhang X, Guo Z. 2019. Preparation and performance testing of superhydrophobic flame retardant cotton fabric. *New Journal of Chemistry* 43(15):5839–48
- Accident Investigation Team of Wuxi Municipal People's Government. 2024. Accident investigation report of Wuxi Tiantianrun Textile Technology Co., Ltd. "11-20" major fire accident. www.fire114.cn/index/slibrary/detail/i/127622.html (Accessed on 11 Jan. 2025)
- Ren Y, Gu Y, Zeng Q, Zhang Y. 2017. UV-induced surface grafting polymerization for preparing phosphorus-containing flame retardant polyacrylonitrile fabric. *European Polymer Journal* 94:1–10
- Wang D, Zhong L, Zhang C, Zhang F, Zhang G. 2018. A novel reactive phosphorous flame retardant for cotton fabrics with durable flame retardancy and high whiteness due to self-buffering. *Cellulose* 25(10):5479–97
- Sykam K, Försth M, Sas G, Restás Á, Das O. 2021. Phytic acid: A bio-based flame retardant for cotton and wool fabrics. *Industrial Crops and Products* 164:113349
- Nguyen Thi H, Hong KVT, Ha TN, Phan DN. 2020. Application of plasma activation in flame-retardant treatment for cotton fabric. *Polymers* 12(7):1575
- Song WM, Zhang LY, Li P, Liu Y. 2023. High-efficient flame-retardant finishing of cotton fabrics based on phytic acid. *International Journal of Molecular Sciences* 24(2):1093
- Alongi J, Carosio F, Malucelli G. 2014. Current emerging techniques to impart flame retardancy to fabrics: an overview. *Polymer Degradation and Stability* 106:138–49
- Liu Y, Ding D, Lu Y, Chen Y, Liao Y, et al. 2022. Efficient and durable cotton fabric surface modification via flame retardant treatment. *Colloids and Surfaces A: Physicochemical and Engineering Aspects* 648:129005
- Zhou S, Yang Y, Zhu Z, Xie Z, Sun X, et al. 2021. Preparation of a halogen-free flame retardant and its effect on the poly(L-lactic acid) as the flame retardant material. *Polymer* 229:124027
- Tan W, Ren Y, Xiao M, Guo Y, Liu Y, et al. 2021. Enhancing the flame retardancy of lyocell fabric finished with an efficient, halogen-free flame retardant. *RSC Advances* 11(55):34926–37
- Mata MC, Castro V, Quintana JB, Rodil R, Beiras R, et al. 2022. Bioaccumulation of organophosphorus flame retardants in the marine mussel *Mytilus galloprovincialis*. *Science of The Total Environment* 805:150384
- Feng Y, Zhou Y, Li D, He S, Zhang F, et al. 2017. A plant-based reactive ammonium phytate for use as a flame-retardant for cotton fabric. *Carbohydrate polymers* 175:636–44
- Luo Q, Wang M, Zhang H, Ouyang Y, Lin H, et al. 2021. Preparation and properties of bio-based flame retardant L-APP/poly(L-lactic acid) composites. *Journal of Renewable Materials* 9(12):2067
- Kumar M, Barbhui MD. 2023. Sustainable fire safety solutions: bioactive natural polysaccharides and secondary metabolites as innovative fire retardants for textiles. *Emergency Management Science and Technology* 3:17
- Liu X, Zhang Q, Peng B, Ren Y, Cheng B, et al. 2020. Flame retardant cellulosic fabrics via layer-by-layer self-assembly double coating with egg white protein and phytic acid. *Journal of Cleaner Production* 243:118641
- Xu Y, Zhang W, Qiu Y, Xu M, Li B, et al. 2022. Preparation and mechanism study of a high efficiency bio-based flame retardant for simultaneously enhancing flame retardancy, toughness and crystallization rate of poly (lactic acid). *Composites Part B: Engineering* 238:109913
- Malucelli G. 2020. Flame-retardant systems based on chitosan and its derivatives: State of the art and perspectives. *Molecules* 25(18):4046
- Alongi J, Carletto RA, Di Blasio A, Carosio F, Bosco F, et al. 2023. DNA: a novel, green, natural flame retardant and suppressant for cotton. *Journal of Materials Chemistry A* 11(15):4779–85
- Wang TC, Jia MH, Xu NT, Hu W, Jiang Z, et al. 2024. Facile fabrication of adenosine triphosphate/chitosan/polyethyleneimine coating for high flame-retardant lyocell fabrics with outstanding antibacteria. *International Journal of Biological Macromolecules* 260:129599
- Sun J, Pang Y, Yang Y, Zhao J, Xia R, et al. 2019. Improvement of rice husk/HDPE bio-composites interfacial properties by silane coupling agent and compatibilizer complementary modification. *Polymers* 11(12):1928
- China National Textile And Apparel Council. 1997. *GB/T 5454-1997: Textiles-Burning behaviour-Oxygen index method*. Beijing: Standards Press of China
- General Administration of Quality Supervision, Inspection and Quarantine of the People's Republic of China. 2014. *GB/T 5455-2014: Textiles-Burning behaviour-Determination of damaged length, afterglow time and afterflame time of vertically oriented specimens*. Beijing: Standards Press of China
- International Organization for Standardization. 2015. *ISO 5660-1: 2015. Reaction to fire tests-Heat release, smoke production and mass loss rate*. Geneva: International Organization for Standardization
- Li G, You F, Zhou S, Wang Z, Li D, et al. 2022. Preparations, characterizations, thermal and flame retardant properties of cotton fabrics finished by boron-silica sol-gel coatings. *Polymer Degradation and Stability* 202:110011

28. Yu J, Pang Z, Zheng C, Zhou T, Zhang J, et al. 2019. Cotton fabric finished by PANI/TiO₂ with multifunctions of conductivity, anti-ultraviolet and photocatalysis activity. *Applied Surface Science* 470:84–90
29. Zhang X, Wang Z, Zhou S, You F, Li D, et al. 2022. Enhanced flame retardancy level of a cotton fabric treated by an ammonium pentaborate doped silica-KH570 sol. *Journal of Industrial Textiles* 52:1–29
30. Lin D, Zeng X, Li H, Lai X, Wu T. 2019. One-pot fabrication of superhydrophobic and flame-retardant coatings on cotton fabrics via sol-gel reaction. *Journal of colloid and interface science* 533:198–206
31. Zhang QH, Gu J, Chen GQ, Xing TL. 2016. Durable flame retardant finish for silk fabric using boron hybrid silica sol. *Applied Surface Science* 387(30):446–53
32. Naik AD, Fontaine G, Samyn F, Delva X, Bourgeois Y, et al. 2013. Melamine integrated metal phosphates as non-halogenated flame retardants: synergism with aluminium phosphinate for flame retardancy in glass fiber reinforced polyamide 66. *Polymer Degradation and Stability* 98:2653–62
33. Zhang L, Li X, Zhang S, Gao Q, Lu Q, et al. 2021. Micro-FTIR combined with curve fitting method to study cellulose crystallinity of developing cotton fibers. *Analytical and Bioanalytical Chemistry* 413:1313–20
34. Yuan H, Xing W, Zhang P, Song L, Hu Y. 2012. Functionalization of cotton with UV-cured flame retardant coatings. *Industrial & Engineering Chemistry Research* 51(15):5394–401
35. Liu Y, Pan YT, Wang X, Acuña P, Zhu P, et al. 2016. Effect of phosphorus-containing inorganic-organic hybrid coating on the flammability of cotton fabrics: Synthesis, characterization and flammability. *Chemical Engineering Journal* 294:167–75
36. Zhou L, Liang Z, Li R, Huang D, Ren X. 2017. Flame-retardant treatment of cotton fabric with organophosphorus derivative containing nitrogen and silicon. *Journal of Thermal Analysis and Calorimetry* 128(2):653–60
37. Ahmad I, Kan CW, Yao Z. 2019. Photoactive cotton fabric for UV protection and self-cleaning. *RSC advances* 9(32):18106–14
38. Ren Y, Huo T, Qin Y, Liu X. 2018. Preparation of flame retardant polyacrylonitrile fabric based on sol-gel and layer-by-layer assembly. *Materials*, 2018,11(4):483
39. Akiyama Y, Sodaye H, Shibahara Y, Honda Y, Tagawa S, et al. 2010. Study on gamma-ray-induced degradation of polymer electrolyte by pH titration and solution analysis. *Polymer Degradation and Stability* 95:1–5
40. Gao D, Zhang Y, Lyu B, Wang P, Ma J. 2019. Nanocomposite based on poly (acrylic acid)/attapulgite towards flame retardant of cotton fabrics. *Carbohydrate polymers* 206:245–53
41. Zhang Q, Huang NH, Xu YC. 2008. Study on the thermal degradation kinetics of cotton fiber. *Journal of Textile Research* 29(2):15–19
42. Liu M, Huang S, Zhang G, Zhang F. 2019. Synthesis of P–N–Si synergistic flame retardant based on a cyclodiphosphazane derivative for use on cotton fabric. *Cellulose* 26(12):7553–67
43. Cheng F, Zhang X, Yang X, Li R, Wu Y. 2021. Research on carbonization kinetic of cellulose-based materials and its application. *Journal of Analytical and Applied Pyrolysis* 158:105232
44. Bourbigot S, Le Bras M, Delobel R. 1995. Fire degradation of an intumescent flame retardant polypropylene using the cone calorimeter. *Journal of fire sciences* 13(1):3–22



Copyright: © 2025 by the author(s). Published by Maximum Academic Press on behalf of Nanjing Tech University. This article is an open access article distributed under Creative Commons Attribution License (CC BY 4.0), visit <https://creativecommons.org/licenses/by/4.0/>.